THE JOURNAL OF PHYSICAL CHEMISTRY B

Article

pubs.acs.org/JPCB

Linkage Isomerization via Geminate Cage or Bimolecular Mechanisms: Time-Resolved Investigations of an Organometallic Photochrome

Kristy M. DeWitt,[†,§] Tung T. To,[†,#] Edwin J. Heilweil,*[,†] and Theodore J. Burkey*[,‡]

[†]Radiation Physics Division, Physical Measurement Laboratory, National Institute of Standards and Technology, Gaithersburg, Maryland 20899-8443, United States

[‡]Department of Chemistry, The University of Memphis, Memphis, Tennessee 38152-3550, United States

Supporting Information

ABSTRACT: The extent of the photoinitiated linkage isomerization of dicarbonyl(3-cyanomethylpyridine-κN)(η^5-methylcyclopentadienyl)manganese (**4**) to dicarbonyl(3-cyano-κN-methylpyridine)(η^5-methylcyclopentadienyl)manganese (**5**) was examined by time-resolved infrared spectroscopy on picosecond to microsecond time scales in room temperature isooctane to determine the extent the isomerization occurs as a geminate cage rearrangement. We previously reported that a substantial part of the conversion between **4** and **5** must be a bimolecular reaction between a solvent coordinated dicarbonyl(η^5-methylcyclopentadienyl)manganese (**3**) and uncoordinated 3-cyanomethylpyridine. For the purpose of designing a molecular device, it would be desirable for the photoisomerization to occur in a geminate cage reaction, because the faster the isomerization, the less opportunity for side reactions to occur. In this study, assignments of transients are identified by comparison with transients observed for model reactions. Within 100 μs after photolysis of **4** in isooctane, no **5** is observed. Instead, the solvent coordinated **3** is observed within 25 ps after irradiation. The formation of **5** is observed only in the presence of 9 mM 3-cyanomethylpyridine but not until 10−50 μs after irradiation of **4**. Within the limits of detection, these results indicate the conversion of **4** to **5** occurs exclusively via a bimolecular reaction of 3-cyanomethylpyridine with solvent coordinated **3** and not a geminate cage reaction between 3-cyanomethylpyridine and the dicarbonyl(η^5-methylcyclopentadienyl)manganese fragment.

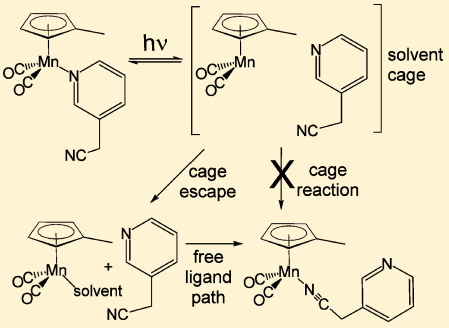

INTRODUCTION

Photochromes have found applications in information processing and data storage with the development of optical switches,[1−4] optical memories,[5−11] three-dimensional data storage,[12] and holographic recording.[13−15] Development has begun in microfabrication,[16] wettability of surfaces (for microfluidic devices),[17] and volume changes (for photoactuators).[18−21] A photochromic response can be achieved with organometallic compounds via a ligand substitution where the coordination of two Lewis bases with different functional groups leads to different chromophores. For example, we find that the dicarbonylmethylcylcopentadienylmanganese complexes with pyridine and acetonitrile are orange and yellow, respectively (Scheme 1).[22] Desirable properties include well-resolved chromophores with corresponding photolabile ligands, high quantum yields for substitution, ultrafast response times, and low fatigue while cycling between color states. The formation of long-lived intermediates can be problematic, since the longer the lifetime of an intermediate the greater the probability of unwanted side reactions. High concentrations of acetonitrile employed in Scheme 1 increase the rates of substitution and reduce the lifetime of **3**, but the reverse photosubstitution would be inhibited by acetonitrile reaction with **3**. Therefore, driving the reaction toward **1** or **2** depends on the relative concentrations of the two Lewis bases as well as the quantum yields and extinction coefficients of **1** and **2**. Such systems are inherently inefficient for multiple cycles between the color states (**1** → **2** → **1**) since increasing the concentration of one ligand increases the yield of substitution in one direction while reducing the yield in the reverse direction.

Scheme 1

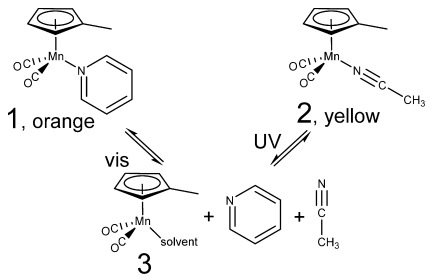

Received: December 31, 2014
Revised: March 18, 2015
Published: March 25, 2015

ACS Publications © 2015 American Chemical Society

DOI: 10.1021/jp513033j
J. Phys. Chem. B 2015, 119, 5531−5536

There have been several studies of photoinduced linkage isomerizations, but most are based on 1,2 migrations that appear to be nondissociative. These include linkage isomerizations of sulfoxide, NO, and NO_2 complexes,[23−27] and results indicate that some isomerizations are caged. We previously speculated that a photoinitiated linkage isomerization with a bifunctional ligand might, in part, occur by a geminate cage reaction and reduce the need for excess ligand to avoid fatigue (Scheme 2, path A).[22] Alternating visible and UV irradiation of

Scheme 2

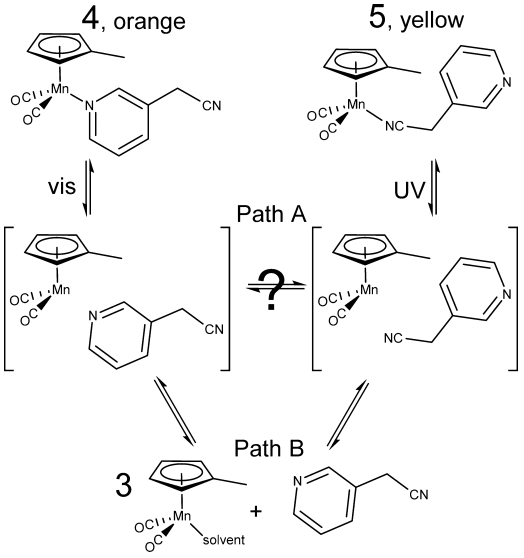

photochrome **4**/**5** produces a photochromic response, but it diminishes with each cycle unless excess ligand is added. This indicates a bimolecular pathway between isomers occurs to some extent, that is, a reaction with a ligand from outside the solvent cage (Scheme 2, path B). Strictly speaking, this pathway is a substitution, not a linkage isomerization. The results neither confirmed nor excluded a caged linkage isomerization. Our group and others have reported photoinduced linkage isomerization for complexes with tethered bifunctional ligands which eliminate ligand escape; however, tethering may introduce adverse strain and propinquity effects.[28−33] To understand how tethering affects linkage isomerization, we are examining the linkage isomerization of untethered ligands. In this study, the time scales and mechanisms for the photochrome conversion **4** → **5** have been investigated using time-resolved infrared (TRIR) spectroscopy to determine the extent geminate linkage isomerization and ligand escape from the solvent cage occur with an untethered bifunctional ligand.

EXPERIMENTAL SECTION

TRIR Spectrometer. Experiments were performed with a home-built, 1 kHz, Ti:sapphire based UV/visible pump dual-beam IR probe femtosecond TRIR spectrometer schematically depicted in the Supporting Information (Figure S1).[34] Broadband mid-infrared probe pulses were obtained with an intracavity-doubled diode-pumped continuous-wave (CW) Nd:YVO_4 laser (Coherent Verdi-V5, 3.5 W, 532 nm) to pump a passively mode locked Ti:sapphire oscillator (Kapteyn-Murnane Laboratories linear cavity). The oscillator output (∼200 mW, 80 MHz repetition rate, 100 fs, centered at 785 nm) was the seed for a home-built Ti:sapphire chirped pulse amplifier composed of a stretcher, compressor, and linear cavity regenerative amplification stage. The amplification stage was pumped by an intracavity-doubled diode-pumped Q-switched Nd:YLF laser (Spectra Physics Evolution-X, 527 nm, 1 kHz, ∼7 mJ/pulse). A single Pockels cell aligned as a static quarter-wave plate was used for switch-in and switch-out of the seed and amplified pulses, respectively. The final output of the amplifier was a 1 kHz train of ∼100 fs (150 cm^{-1}) pulses, centered at 785 nm (800 μJ/pulse). An optical parametric amplifier (Spectra-Physics OPA-800C) converted the amplified Ti:sapphire output to tunable mid-infrared pulses. Dual pass optical parametric generation−amplification in a β-barium borate (BBO) crystal produced a near-infrared signal and idler pulses which were collinearly combined in $AgGaS_2$ to produce broadband mid-infrared probe pulses via difference frequency generation (DFG). An 800 nm dielectric mirror separated residual 785 nm light after the BBO crystal for use as excitation pulses (see below), and a long-pass filter blocked any residual signal and idler after the DFG crystal. The DFG power was ∼2 μJ/pulse near 2000 cm^{-1} (5 μm wavelength) with ca. 100 fs pulse duration and usable bandwidth of 200 cm^{-1} fwhm.

Excitation Pulse Generation. For experiments where the probe delay was <400 ps, pump pulses were generated from the residual 785 nm output (85 fs duration, ∼400 μJ/pulse) left over after the OPA parametric process used to make signal and idler pulses. This beam was separated from the near-IR beams with a 45° dielectric mirror−filter. Visible pump pulses (393 nm, ∼60 μJ/pulse) were produced by frequency doubling in type I BBO. UV excitation pulses (262 nm, ∼10 μJ/pulse) were generated by sum frequency generation (SFG) between the doubled light and residual 785 nm light, also in type I BBO. A $\lambda/2$ waveplate was used to rotate the polarization of the 785 nm light 90° prior to the second BBO crystal. A wavelength-dependent delay plate was also used before the second crystal to improve temporal overlap between the 785 and 393 nm beams in order to maximize the 262 nm energy conversion efficiency. Dichroic mirrors were used after the mixing crystals to separate the desired excitation wavelength which was combined with the IR probe beam before the sample.

For experiments with pump/probe delay ranging from 50 ns to 400 μs, a second kilohertz amplified Ti:sapphire system, electronically synchronized to the one described above, was used to generate the pump pulses. In this system, seed pulses were produced by a Ti:sapphire oscillator (Coherent Mira, 76 MHz, 35 fs, 500 mW, centered 800 nm) pumped by a CW diode-pumped intracavity-doubled Nd:YVO_4 (Coherent Verdi-V5, 532 nm, 5 W). The seed pulses were amplified in a Ti:sapphire chirped-pulse amplifier (Positive Light Legend HE) pumped by a intracavity-doubled diode-pumped Q-switched Nd:YLF (Positive Light Evolution 30, 527 nm, 17 W). The final output of the amplifier was a 1 kHz train of ∼45 fs pulses, centered at 800 nm, with a pulse energy of 2 mJ/pulse. Half of this energy was used to generate pump pulses for the TRIR experiments. Visible (400 nm, 60 μJ/pulse) and UV (267 nm, 20 μJ/pulse) pulses were produced in the same BBO mixing crystals by doubling and SFG, as described previously. To obtain UV pulses for long time delays, the full power of the 800 nm beam was used, but to generate visible light, absorptive neutral density filters were placed in the 800 nm beam to limit the 400 nm energy to 60 μJ/pulse. This was done to prevent window damage and sample degradation due to two-photon absorption processes. Pulse jitter between the nanosecond electronically delayed systems was at most ∼25 ns (originating

DOI: 10.1021/jp513033j
J. Phys. Chem. B 2015, 119, 5531−5536

from the two unlocked seed oscillators) arising from countdown circuitry controlling the two laser systems' Pockels cells used to inject and reject amplified seed pulses.

The mid-IR beam generated by the OPA passed through a computer-controlled variable optical delay stage (up to 450 ps) and was split by a broadband 50% IR beamsplitter into probe and reference beams. These two beams were aligned parallel and approximately 1 cm apart onto a beam combiner (1 mm thick sapphire flat with a 100% visible or UV reflection dielectric coating) to make the broadband infrared probe and UV/vis pump beams collinear. All three beams were then focused by a 25.4 mm diameter, 10 cm focal length CaF_2 lens into the liquid sample cell and subsequently recollimated by a matched 10 cm CaF_2 lens. The sample cell was positioned at the IR focus and, due to achromaticity, slightly beyond the UV/vis pump pulse focus. A periscope was used to "flip" the horizontally separated beams into a pair of vertically separated beams, which were focused with a 15 cm focal length CaF_2 lens onto the slit of a 1/4 m Czerny–Turner monochromator with a 70 grooves/mm ruled grating optimized for 5 μm wavelength. In the monochromator, the signal and reference beams were chromatically separated on discrete "slices" of the grating. After the monochromator's exit slit, the signal and reference beams were separately focused onto the active elements of a matched pair of liquid nitrogen cooled HgCdTe detectors (Graseby HCT-5-1.0, D^* optimized for 5 μm, 1 mm^2 active elements). Bias voltage for the photoconductive detectors and ~1000× signal gain was provided by a pair of preamplifiers (Infrared Associates DP-8000). Si wafers placed in front of the HgCdTe detectors blocked stray UV or visible light from reaching the active elements, but allowed mid-IR light to pass to the detectors. The entire TRIR spectrometer was enclosed in an acrylic box allowing it to be purged with dry air to eliminate IR absorption by gas phase water and carbon dioxide. The major bleach and absorption features discussed below were found to respond linearly to applied pump pulse intensity.

Signal Acquisition and Processing. A double-pulse generator produced a 2 kHz trigger signal synchronized to the native 1 kHz repetition rate of the laser systems. Data from the amplified HgCdTe detectors was obtained at 2 kHz with gated boxcar averagers (Stanford Research SR250), recorded using the analog voltage inputs of a PCI-slot data acquisition card (NI-DAQ PCI-6034E), and processed with a program written in Visual Basic. The "laser-off" data collected between "IR-on" shots was used to correct for background drift and 60 Hz line noise. For each "IR-on" shot, the signal channel was divided by the reference channel to normalize shot-to-shot amplitude fluctuations. The UV/vis pump beam was chopped at 500 Hz by a phase-synchronized optical chopper. A Si photodiode, sampled by a third boxcar averager, monitored scattered pump light to correlate the phase of the optical chopper with the recorded HgCdTe output data. After obtaining the "pump-off" data (T_{off}) from the "pump-on" data (T_{on}), computing $-\log_{10}(T_{off} - T_{on})$ converted the measured voltages to an absolute change in optical density. TRIR spectra were obtained by fixing a specific pump/probe time delay, either by moving the optical delay on the IR beam (picosecond experiments) or the electronic delay separating the two Ti:sapphire systems (nanosecond to microsecond experiments) and then step-scanning the monochromator across a desired spectral wavelength range. A scan of a TRIR difference spectrum was obtained by stepping the monochromator at 1 cm^{-1}/s while averaging 1000 laser shots/s where a scan of 300 cm^{-1} took approximately 5 min.

Sample Preparation. Dicarbonyl(3-cyanomethylpyridine-κN)(η^5-methylcyclopentadienyl)manganese (**4**) was prepared by a published procedure.[1] **4** was shielded from ambient light during all procedures. In a typical experiment, **4** (50 mg) in 100 mL of isooctane (Aldrich, ACS spectrophotometric grade) was prepared under argon and dissolved by sonication for 10 min. Fresh **4** solutions (20 mL) were used for each TRIR scan. **5** solutions were likewise prepared and then exposed to continuous room light before TRIR experiments. Tricarbonylmethylcyclopentadienylmanganese (TMM) solutions (0.8 mM in heptane and isooctane) were prepared in air. Solutions were irradiated in a stainless steel flow cell with 2 mm thick CaF_2 windows separated by 1 or 3 mm with Teflon spacers. During irradiation, the solutions were circulated through a closed Teflon–stainless steel flow system containing the cell, a reservoir, and a magnetic-drive pump. For all experiments, the flow system was purged with dry Ar during and for at least 2 h prior to data collection.

RESULTS AND DISCUSSION

Previous studies demonstrate that the weakest Mn–L bond dissociates in dicarbonylcyclopentadienylmanganese derivatives. For example, pyridine dissociates while strongly bonding phosphines do not.[35,36] In a previous study we observed the interconversion of **4** and **5** in isooctane by Fourier transform infrared (FTIR) spectroscopy during steady-state irradiation.[22] The symmetric and asymmetric CO-stretching absorption bands of **4** appear at 1933 and 1868 cm^{-1}, respectively, while the CN stretch absorbs at 2255 cm^{-1}. Visible irradiation depletes the **4** absorption bands while new CO-stretching absorption bands appear for **5** at 1943 and 1885 cm^{-1} in addition to a coordinated CN-stretching absorption band at 2025 cm^{-1}.

Figure 1 shows TRIR data for 0.8 mM **4** in isooctane using 393 or 400 nm irradiation with pump/probe delays ranging from the picosecond to microsecond time scales. Bleach bands at 1933 and 1868 cm^{-1} correspond to loss of the parent compound. In the picosecond data, a single transient absorption band at 1988 cm^{-1} appears at early time, decaying with a time constant of approximately 100 ps. We do not know

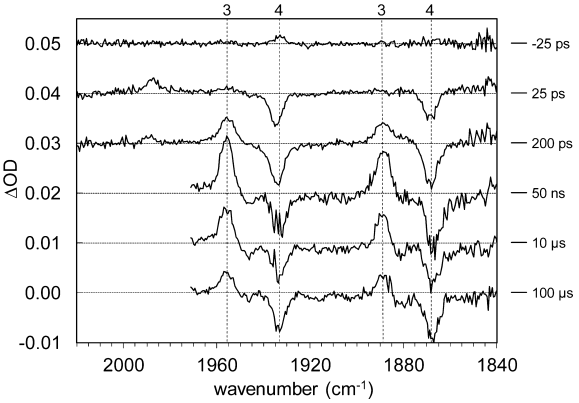

Figure 1. TRIR difference spectra for irradiation at 393 nm with 1 mm path length (<1 ns) or 400 nm with 3 mm path length (>1 ns) of 0.8 mM **4** in isooctane at 293 K. All spectra are single scans with 0.01 OD offset. A figure with additional time delays is reported in the Supporting Information (Figure S3).

DOI: 10.1021/jp513033j
J. Phys. Chem. B 2015, 119, 5531–5536

the precise origin of this transient carbonyl absorption band, but it is similar to the peak assigned to a transient radical triplet state or twisted Cp ligand configuration for dicarbonyl-(cyclopentadienyl)]manganese (no methyl group).[37,38] On the same time scale as this transient band disappears, two strong absorption bands grow in at 1955 and 1888 cm^{-1} *which do* ***not*** *correspond to the direct formation of* **5** (see below). These absorptions are assigned to isooctane coordinated [dicarbonyl-(methylcyclopentadienyl)]manganese consistent with previous observations of alkane coordinated [dicarbonyl-(cyclopentadienyl)]manganese complexes.[37,39] There is no evidence of nitrile-coordinated CO-stretch absorption bands expected for **5** at 1943 or 1885 cm^{-1} which should persist beyond the microsecond time scale. In the nanosecond to microsecond data, over the time span of 50 ns−100 μs, no changes are observed in the TRIR spectrum except for a slow decrease in overall signal intensity and hints of very small bleach bands at 1943 and 1885 cm^{-1}. The intensity decrease is attributed to photoinduced transients flowing out of the beam volume before the probe pulse interrogates the sample. The frequencies of the small bleach bands are consistent with the loss of **5** that had formed previously in the recycled irradiated solution. We suspect the high intensity of the ∼45 fs, 393 nm pump pulses produces a small amount of two-photon excitation of **5**; therefore, a bleach band for **5** is observed.

Previous studies establish that CO dissociates upon irradiation of TMM (tricarbonylmethylcyclopentadienylmanganese) and the dicarbonylmethylcyclopentadienylmanganese fragment coordinates alkane solvents (Scheme 3).[36,40] Exami-

Scheme 3

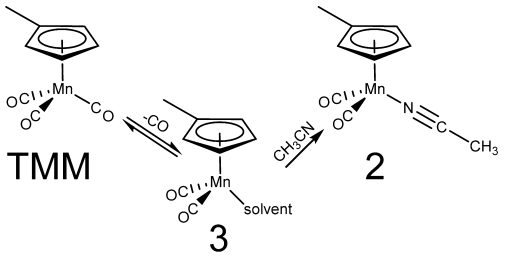

nation of the TRIR spectra following irradiation of TMM provides confirmation of the transient species assigned following irradiation of **4** (Figure 2). The single bleach feature near 2017 cm^{-1} and the unresolved doublet bleach near 1943 cm^{-1} correspond to loss of the TMM after UV irradiation in isooctane.[35] Bands at 1988, 1955 (overlapping), and 1888 cm^{-1} were also observed after irradiation of **4**. The solvent is the only species available to react within 100 ps following UV irradiation of TMM, and it is well-established that an alkane coordinated complex such as **3** is formed following UV irradiation of TMM.[36−38] Thus, the appearance of 1955 and 1888 cm^{-1} dicarbonyl absorption bands after irradiation of **4** confirm the formation of **3**. Like Figure 1, the 1988 cm^{-1} band in Figure 2 appears within 25 ps and decays with ca. 100 ps lifetime as the 1955 and 1888 cm^{-1} bands grow. While no peaks grow between 200 ps and 100 μs, there is a slow decay of all peaks which is attributed to the flow of irradiated solution out of the beam path and reaction of CO with **3**. In contrast, following irradiation of TMM in the presence of acetonitrile in heptane, the 1955 and 1888 cm^{-1} bands of **3** decay between 1 and 100 μs as the 1880 cm^{-1} band assigned to the nitrile product **2** grows (Figure 3). The growth of a 1943 cm^{-1} band for **2** is

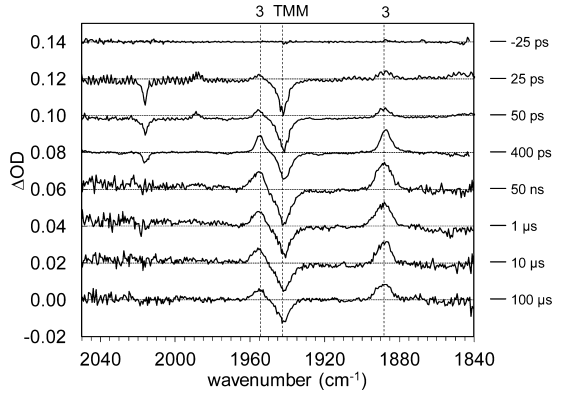

Figure 2. TRIR difference spectra for irradiation at 393 nm (<1 ns, average of three scans) or 400 nm (>1 ns, two scans) of 0.8 mM TMM in isooctane at 293 K with 1 mm path length. Spectra have 0.02 OD offset. A figure with additional time delays is reported in the Supporting Information (Figure S4).

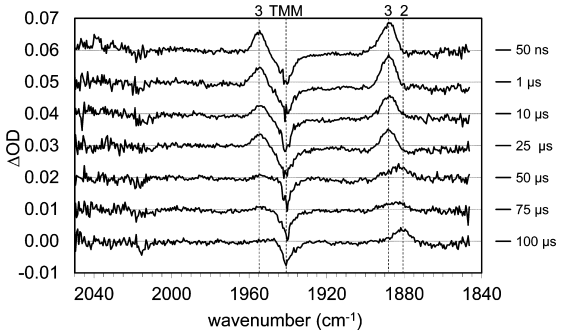

Figure 3. TRIR difference spectra after irradiation at 400 nm of 0.8 mM TMM and 1.6 mM acetonitrile in isooctane at 293 K with 1 mm path length. Spectra are single scans with 0.01 OD offset.

obscured by overlap with the TMM bleach, and evidence of its growth is the decrease in the corresponding TMM bleach intensity. The 2025 cm^{-1} band for **2** is obscured by the TMM bleach and noise.

Even at 100 μs after irradiation of **4** there was no evidence in Figure 1 of bands near 1943 and 1885 cm^{-1} like those observed for **2** in Figure 3 that could be attributed to **5** nor was there recovery of **4** bleaches at 1933 and 1868 cm^{-1}. The amount of 3-cyanomethylpyridine liberated upon irradiation of **4** was apparently too low to react with **3** within 100 μs. In contrast to Figure 1, TRIR spectra following the 400 nm irradiation of **4** with 10-fold excess 3-cyanomethylpyridine exhibits decay of the 1955 and 1888 cm^{-1} bands for **3** between 50 ns and 50 μs as bands at 1947 and 1885 cm^{-1} grow (Figure 4).[41] These bands which are assigned to the linkage isomer **5** are similar to the bands near 1943 and 1880 cm^{-1} for **2** at 100 μs delay (Figure 3). There also appears to be a partial recovery of the **4** bleach bands at 1933 and 1868 cm^{-1} that is attributed to reformation of **4** in competition with the formation of **5** and nonirradiated solution entering the excitation volume.

Figure 5 shows TRIR data for 0.8 mM **5** in isooctane using UV pump irradiation with pump/probe delays on nanosecond to microsecond time scales. Bleach bands at 1947 and 1885 cm^{-1} correspond to loss of **5**, while new transient absorbances at 1955 and 1888 cm^{-1} correspond to formation of the same solvent-coordinated intermediate observed after visible irradiation of **4**. Since no **4** is observed at 50 ns, a measurable amount of linkage isomerization in the solvent cage did not

DOI: 10.1021/jp513033j
J. Phys. Chem. B 2015, 119, 5531−5536

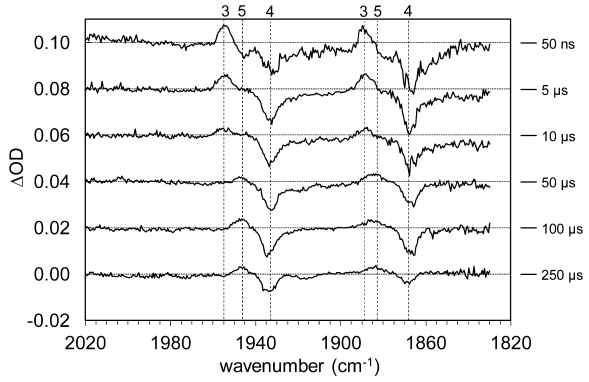

Figure 4. TRIR difference spectra for irradiation at 400 nm with 1 mm path length of 0.8 mM **4** and 9 mM 3-cyanomethylpyridine in isooctane. All spectra are single scans with 0.02 OD offset.

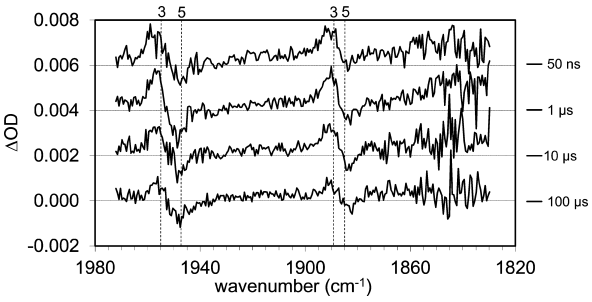

Figure 5. TRIR difference spectra for irradiation at 267 nm with 1 mm path length of 0.8 mM **5** in isooctane at 293 K. All spectra are the average of three single scans with 0.02 OD offset.

occur since only the solvent coordinated complex **3** was observed. Unfortunately, adding 10 times excess 3-cyanomethylpyridine to the solution of **5** in a similar experiment absorbed most of the UV pump light, making it impossible to achieve enough excitation of **5** to observe transients.

CONCLUSIONS

We previously suggested that the photolysis of **4** could form the linkage isomer **5** by two pathways: isomerization in the solvent cage and reaction of the solvent coordinated **3** with free ligand. If a linkage isomerization of **4** occurs by a geminate cage reaction, then **5** should appear within 100 ps. Instead, only the solvent coordinated complex **3** is observed. The linkage isomer only appears after 5 μs if 3-cyanomethylpyridine is present in large excess: the coordinated solvent of **3** is displaced by the cyano group of 3-cyanomethylpyridine in competition with the pyridinyl group. Within the limits of detection, we conclude that the isomer forms exclusively by a second-order substitution reaction and not a cage rearrangement. Strictly speaking, the reaction is a substitution, not a linkage isomerization, since **5** does not contain all the original atoms from **4**. The results are consistent with the escape of 3-cyanomethylpyridine from the solvent cage being much faster than a rotation that would bring the cyano group near the metal center. Almost certainly there are collisions of the geminate pair, but these only lead to reforming the starting material **4** or the solvent coordinated **3**.

For the exchange of pyridinyl and nitrile functional groups, the reaction of Scheme 2 is no more effective than that in Scheme 1: both occur by a bimolecular processes. Furthermore, there appears to be little benefit to create a photochrome by connecting two functional groups in this case. We do not anticipate complexes with untethered bifunctional ligands will be useful for practical applications, but discovering what structural features favor cage linkage isomerization should assist in the design of efficient tethered systems. To our knowledge, photoinduced, caged linkage isomerizations based on 1,3 and longer bond migrations have not been reported. We recently prepared a dicarbonylcyclopentadienylmanganese complex with two groups tethered to the cyclopentadienyl ring that undergo a linkage isomerization (1,4 bond migration by the metal) in less than 100 ps with no competing ultrafast solvent coordination.[42]

ASSOCIATED CONTENT

Supporting Information

Diagram of TRIR spectrometer; TRIR and FTIR spectra of TMM with acetonitrile. This material is available free of charge via the Internet at http://pubs.acs.org.

AUTHOR INFORMATION

Corresponding Authors

*E-mail: edwin.heilweil@nist.gov (E.J.H.).
*E-mail: tburkey@memphis.edu (T.J.B.).

Present Addresses

[§]K.M.D.: IARPA Smart Collection, Intelligence Advanced Research Projects Activity, Washington, DC 20511, USA.
[#]T.T.T.: Acoustics Laboratory, Blachford Inc., 1445 Powis Rd., West Chicago, IL 60185, USA.

Notes

The authors declare no competing financial interest.

ACKNOWLEDGMENTS

This work was partially supported by the National Science Foundation under Grant CHE0911528. Partial support was provided to E.J.H. and T.T.T. for their contributions through internal NIST Scientific, Technical and Research Services (STRS) funds, and K.M.D. gratefully acknowledges support through a NIST National Research Council postdoctoral associateship position.

REFERENCES

(1) Irie, M. Photochromism: Memories and Switches. *Chem. Rev.* **2000**, *100*, 1683−1684.
(2) Willner, I. Photoswitchable Biomaterials: En Route to Optobioelectronic Systems. *Acc. Chem. Res.* **1997**, *30*, 347−356.
(3) Cinelli, R. A. G.; Pellegrini, V.; Ferrari, A.; Faraci, P.; Nifosi, R.; Tyagi, M.; Giacca, M.; Beltram, F. Green Fluorescent Proteins as Optically Controllable Elements in Bioelectronics. *Appl. Phys. Lett.* **2001**, *79*, 3353−3355.
(4) Raymo, F. N.; Giordani, S. All-Optical Processing with Molecular Switches. *Proc. Natl. Acad. Sci. U.S.A.* **2002**, *99*, 4941−4944.
(5) Myles, A. J.; Branda, N. R. Novel Photochromic Homopolymers Based on 1,2-Bis(3-thienyl)cyclopentenes. *Macromolecules* **2003**, *36*, 298−303.
(6) Heller, H. G. The Development of Photochromic Compounds for use in Optical Information Store. *Chem. Ind. (London)* **1978**, 193−196.
(7) Tsivgoulis, G. M.; Lehn, J. M. Photonic Molecular Devices: Reversibly Photoswitchable Fluorophores for Nondestructive Readout for Optical Memory. *Angew. Chem., Int. Ed. Engl.* **1995**, *34*, 1119−1122.
(8) Tyson, D. S.; Bignozzi, C. A.; Castellano, F. N. Metal−Organic Approach to Binary Optical Memory. *J. Am. Chem. Soc.* **2002**, *124*, 4562−4563.

DOI: 10.1021/jp513033j
J. Phys. Chem. B 2015, 119, 5531−5536

(9) Tsujioka, T.; Kondo, H. Organic Bistable Molecular Memory using Photochromic Diarylethene. *Appl. Phys. Lett.* **2003**, *83*, 937−939.
(10) Murakami, M.; Miyasaka, H.; Okada, T.; Kobatake, S.; Irie, M. Dynamics and Mechanisms of the Multiphoton Gated Photochromic Reaction of Diarylethene Derivatives. *J. Am. Chem. Soc.* **2004**, *126*, 14764−14772.
(11) Myles, A. J.; Branda, N. R. 1,2-Dithienylethene Photochromes and Non-destructive Erasable Memory. *Adv. Funct. Mater.* **2002**, *12*, 167−173.
(12) Parthenopoulos, D. A.; Rentzepis, P. M. Three-Dimensional Optical Storage Memory. *Science* **1989**, *245*, 843−845.
(13) Weiss, V.; Friesem, A. A.; Krongauz, V. A. Holographic Recording and All-Optical Modulation in Photochromic Polymers. *Opt. Lett.* **1993**, *18*, 1089−1091.
(14) Akella, A.; Sochava, S. L.; Hesselink, L. Synthesis and Characterization of Photochromic Organic Films for Holographic Recording. *Opt. Lett.* **1997**, *22*, 919−921.
(15) Dieckmann, V.; Eicke, S.; Springfeld, K.; Imlau, M. Transition Metal Compounds Towards Holography. *Materials* **2012**, *5*, 1155−1175.
(16) Ebisawa, F.; Hoshino, M.; Sukegawa, K. Self-Holding Photochromic Polymer Mach−Zehnder Optical Switch. *Appl. Phys. Lett.* **1994**, *65*, 2919−2921.
(17) Rosario, R.; Gust, D.; Hayes, M.; Jahnke, F.; Springer, J.; Garcia, A. A. Photon-Modulated Wettability Changes on Spiropyran-Coated Surfaces. *Langmuir* **2002**, *18*, 8062−8069.
(18) Ikeda, T.; Nakano, M.; Yu, Y.; Tsutsumi, O.; Kanazawa, A. Anisotropic Bending and Unbending Behavior of Azobenzene Liquid-Crystalline Gels by Light Exposure. *Adv. Mater.* **2003**, *15*, 201−205.
(19) Yu, Y.; Nakano, M.; Ikeda, T. Photomechanics: Directed Bending of a Polymer Film by Light. *Nature* **2003**, *425*, 145.
(20) Athanassiou, A.; Kalyva, M.; Lakiotaki, K.; Georgiou, S.; Fotakis, C. All-Optical Reversible Actuation of Photochromic-Polymer Microsystems. *Adv. Mater.* **2005**, *17*, 988−992.
(21) Jin, Y.; Paris, S. I. M.; Rack, J. J. Bending Materials with Light: Photoreversible Macroscopic Deformations in a Disordered Polymer. *Adv. Mater.* **2011**, *23*, 4312−4317.
(22) To, T. T.; Barnes, C. E.; Burkey, T. J. Bistable Photochromic Organometallics based on Linkage Isomerization: Photochemistry of Dicarbonyl(η^5-methylcyclopentadienyl)manganese(I) Derivatives with a Bifunctional Nonchelating Ligand. *Organometallics* **2004**, *23*, 2708−2714.
(23) King, A. W.; Jin, Y.; Engle, J. T.; Ziegler, C. J.; Rack, J. J. Sequential Picosecond Isomerizations in a Photochromic Ruthenium Sulfoxide Complex Triggered by Pump-Repump-Probe Spectroscopy. *Inorg. Chem.* **2013**, *52*, 2086−2093.
(24) King, A. W.; McClure, B. A.; Jin, Y.; Rack, J. J. Investigating the Effects of Solvent on the Ultrafast Dynamics of a Photoreversible Ruthenium Sulfoxide Complex. *J. Phys. Chem. A* **2014**, *118*, 10425−10432.
(25) Hatcher, L. E.; Christensen, J.; Hamilton, M. L.; Trincao, J.; Allan, D. R.; Warren, M. R.; Clarke, I. P.; Towrie, M.; Fuertes, S.; Wilson, C. C.; Woodall, C. H.; Raithby, P. R. Steady-State and Pseudo-Steady-State Photocrystallographic Studies on Linkage Isomers of [Ni(Et_4dien)(η^2-O,ON)(η^1-NO_2)]: Identification of a New Linkage Isomer. *Chem.—Eur. J.* **2014**, *20*, 3128−3134.
(26) Lee, J.; Kovalevsky, A. Y.; Novozhilova, I. V.; Bagley, K. A.; Coppens, P.; Richter-Addo, G. B. Single- and Double-Linkage Isomerism in a Six-Coordinate Iron Porphyrin Containing Nitrosyl and Nitro Ligands. *J. Am. Chem. Soc.* **2004**, *126*, 7180−7181.
(27) Schaniel, D.; Nicoul, M.; Woike, T. Ultrafast Reversible Ligand Isomerisation in Na_2[Fe(CN)$_5$NO]·$2H_2O$ Single Crystals. *Phys. Chem. Chem. Phys.* **2010**, *12*, 9029−9033.
(28) To, T. T.; Heilweil, E. J.; Duke, C. B., III; Ruddick, K. R.; Webster, C. E.; Burkey, T. J. The Development of Ultrafast Photochromic Organometallics and Photoinduced Linkage Isomerization of Arene Chromium Carbonyl Derivatives. *J. Phys. Chem. A* **2009**, *113*, 2666−2676.
(29) To, T. T.; Duke, C. B.; Junker, C. S.; O'Brien, C. M.; Ross, C. R.; Barnes, C. E.; Webster, C. E.; Burkey, T. J. Linkage Isomerization as a Mechanism for Photochromic Materials: Cyclopentadienylmanganese Tricarbonyl Derivatives with Chelatable Functional Groups. *Organometallics* **2008**, *27*, 289−296.
(30) Kelbysheva, E. S.; Ezernitskaya, M. G.; Strelkova, T. V.; Borisov, Y. A. Photochemistry of π- and n-Donor Bifunctional Monosubstituted Derivatives of Cyclopentadienylmanganese Tricarbonyl Complexes Containing an Allyl Group and Photo- and Thermoisomerization of the Corresponding Dicarbonyl Chelates. *Organometallics* **2011**, *30*, 4342−4353.
(31) McClure, B. A.; Rack, J. J. Two-Color Reversible Switching in a Photochromic Ruthenium Sulfoxide Complex. *Angew. Chem., Int. Ed.* **2009**, *48*, 8556−8558.
(32) McClure, B. A.; Rack, J. J. Ultrafast Spectroscopy of a Photochromic Ruthenium Sulfoxide Complex. *Inorg. Chem.* **2011**, *50*, 7586−7590.
(33) Mockus, N. V.; Rabinovich, D.; Petersen, J. L.; Rack, J. J. Femtosecond Isomerization in a Photochromic Molecular Switch. *Angew. Chem., Int. Ed.* **2008**, *47*, 1458−1461.
(34) We identify certain commercial equipment, instruments, or materials in this article to specify adequately the experimental procedure. In no case does such identification imply recommendation or endorsement by the National Institute of Standards and Technology, nor does it imply that the materials or equipment are necessarily the best available for the purpose.
(35) Giordano, P. J.; Wrighton, M. S. Photodissociation Behavior of dicarbonyl(η^5-cyclopentadienyl) Pyridinomaganese and -Rhenium and Related Complexes. *Inorg. Chem.* **1977**, *16*, 160−166.
(36) Sorenson, A. A.; Yang, G. K. Small-Ring Organometallic Systems. Ring Strain and Quantum Yields of Formation in Manganese Complexes CpMn(CO)(η^2-P-P). *J. Am. Chem. Soc.* **1991**, *113*, 7061−7063.
(37) Yang, H.; Kotz, K. T.; Asplund, M. C.; Harris, C. B. Femtosecond Infrared Studies of Silane Silicon−Hydrogen Bond Activation. *J. Am. Chem. Soc.* **1997**, *119*, 9564−9565.
(38) Yang, H.; Asplund, M. C.; Kotz, K. T.; Wilkens, M. J.; Frei, H.; Harris, C. B. Reaction Mechanism of Silicon−Hydrogen Bond Activation Studied Using Femtosecond to Nanosecond IR Spectroscopy and Ab Initio Methods. *J. Am. Chem. Soc.* **1998**, *120*, 10154−1065.
(39) Peaks occur at 1962 and 1894 cm^{-1} in heptane and 1953 and 1893 cm^{-1} in cyclopentane, both for dicarbonyl(η^5-methylcyclopentadienyl)manganese: Childs, G. I.; Colley, C. S.; Dyer, J.; Grills, D. C.; Sun, X.-Z.; Yang, J. X.; George, M. W. Investigation into the Reactivity of M(η^5-C_5R_5)$(CO)_2$(alkane) (M = Mn or Re; R = H, Me or Ph; Alkane = n-Heptane or Cyclopentane) and Re(η^5-C_5H_5)$(CO)_2$(Xe) in Solution at Cryogenic and Room Temperature. *J. Chem. Soc., Dalton Trans.* **2000**, 1901−1906.
(40) Jiao, T.; Pang, Z.; Burkey, T. J.; Johnston, R. F.; Heimer, T. A.; Kleinman, V. D.; Heilweil, E. J. Ultrafast Ring Closure Energetics and Dynamics of Cyclopentadienyl Manganese Tricarbonyl Derivatives. *J. Am. Chem. Soc.* **1999**, *121*, 4618−4624.
(41) As an additional precaution, the isooctane was dried overnight with molecular sieves to minimize water contamination.
(42) Lubet, P. P.; Johnson, J. O. Alberding, B.; Heilweil, E. J; Burkey, T. J. Manuscript in preparation.

DOI: 10.1021/jp513033j
J. Phys. Chem. B 2015, 119, 5531−5536